

### Comment on "Conditions for Maximum Power Transfer"\*

In recent correspondences by Shulman,<sup>1</sup> Castagnetto and Matheau,<sup>2</sup> there are discussions of the conditions for maximum power transfer. In Shulman's notation, the source impedance is  $Z_s = R_s + jX_s = R_s(1 + jx_s)$ , the load impedance is  $Z = R + jX = R_s(r + jx)$ ,  $P$  is the power delivered to the load, and  $P_0$  is the maximum power available from the source. A very simple procedure is to plot  $Z' = r + j(x + x_s)$  on a Smith Chart. Maximum power transfer occurs when  $Z'$  is the closest to the center of the chart. In other words, maximum power transfer occurs when

$$\Gamma = \left| \frac{r + j(x + x_s) - 1}{r + j(x + x_s) + 1} \right|$$

is minimized, because

$$1 - \Gamma^2 = P/P_0.$$

H. F. MATHIS  
North American Aviation, Inc.  
Columbus, Ohio

\* Received June 17, 1963.

<sup>1</sup> Carl Shulman, "Conditions for maximum power transfer," *IRE TRANS. ON MICROWAVE THEORY AND TECHNIQUES (Correspondence)*, vol. MTT-9, pp. 453-454, September, 1961.

<sup>2</sup> L. Castagnetto, J. C. Matheau, and Carl Shulman, "Some remarks concerning 'Conditions for maximum power transfer,'" *IEEE TRANS. ON MICROWAVE THEORY AND TECHNIQUES (Correspondence)*, vol. MTT-11, pp. 153-154; March, 1963.

### Graphical Analysis of $Q$ Circuits\*

The parameters of a resonator which is coupled to a transmission line can be determined in a straightforward way from the measurement of the reflectance on the line.<sup>1-5</sup> However, graphical methods of evaluating the resonator parameters are based on the assumption that the inductance of the coupling loop can be neglected in comparison with the involved impedances. A simple method of graphical evaluation of the resonator parameters which takes into account the coupling inductance too will be described here.

The need for such a method arose in the course of the development of a wavemeter which had a resistance  $R_L$  in series with the coupling loop. The input reflectance in the detuned short position is shown on Fig. 1. It is seen that the  $Q$  circle does not have its center on the real axis.

\* Received May 20, 1963.

<sup>1</sup> L. R. Walker, "Output circuits," in "Microwave Magnetrons," G. B. Collins, Ed., McGraw-Hill Book Co., Inc., New York, N. Y., ch. 5, pp. 171-187; 1948.

<sup>2</sup> L. Malter and G. R. Brewer, "Microwave  $Q$  measurements in the presence of series losses," *J. Appl. Phys.*, vol. 20, pp. 918-925; October, 1949.

<sup>3</sup> E. L. Ginzton, "Microwave Measurements," McGraw-Hill Book Co., Inc., New York, N. Y.; 1957. See especially, ch. 9.

<sup>4</sup> A. Singh, "An improved method for the determination of  $Q$  of cavity resonators," *IRE TRANS. ON MICROWAVE THEORY AND TECHNIQUES*, vol. MTT-6, pp. 155-160; April, 1958.

<sup>5</sup> E. L. Ginzton, "Microwave  $Q$  measurements in the presence of coupling losses," *IRE TRANS. ON MICROWAVE THEORY AND TECHNIQUES*, vol. MTT-6 pp. 383-389 October, 1958.

Fig. 2 shows the equivalent circuit for the case under investigation. The position of the minimum voltage for the detuned resonator is marked with  $b-b$ , the detuned short position. The reflectances measured on the slotted line in the reference plane  $b-b$  produce the  $Q$  circle on the Smith Chart, denoted  $C_1$  in Fig. 3. Its radius  $r_1$  can be measured on the  $\Gamma$  scale which is usually added to the Smith Chart. The center of the  $Q$  circle is denoted  $S_1$  while  $S_0$  denotes the center of the Smith Chart.

The first step in the graphical analysis under consideration is to determine the circle  $C_2$  which tangentially touches the unit circle (circumference of the Smith Chart) and the  $Q$  circle in the point  $F_\infty$ . The easiest way of locating the circle  $C_2$  is by simple trial. The straight line through points  $F_\infty$  and  $S_1$  is drawn and the point  $S_2$  is located, which makes  $F_\infty S_2 = S_2 A$ .  $A$  is the touching point of the circle  $C_2$  with the unit circle. The circle  $C_2$  with the radius

$r_2$  is thus obtained. The series resistance  $R_1$  in the coupling circuit is given by the relation

$$R_1 = R_K \left( \frac{1}{r_2} - 1 \right), \quad (1)$$

where  $R_K$  denotes the characteristic resistance of the slotted line.

The coupling coefficient  $\kappa$  is here defined as the ratio of coupled resistance to cavity resistance. This corresponds to the situation described by Ginzton<sup>3</sup> in his Figure 9.3d. The coupling coefficient can be determined from the radii  $r_1$  and  $r_2$

$$\kappa = \frac{r_1}{r_2 - r_1}. \quad (2)$$

Note that it is irrelevant whether the  $Q$  circle is overcoupled or undercoupled. All the relations given here are valid for both cases.

The straight line  $f-f$  drawn through  $S_2$  perpendicularly to the line  $F_\infty S_1$  is provided with a linear frequency scale. The particular frequency  $f_0$  is determined by projecting on the scale  $f-f$  the point  $F_0$  out of the point  $F_\infty$ . The frequency  $f_0$ , corresponding to  $F_0$ , is the resonant frequency of the loaded resonator.

By drawing two straight lines through the point  $F_\infty$  at  $45^\circ$  to the line  $F_\infty S_1$ , one obtains the points  $F_1$  and  $F_2$ . The corresponding frequencies  $f_1$  and  $f_2$  are then determined on the frequency scale  $f-f$ . The  $Q$  value of the loaded resonator follows from the familiar expression

$$Q_L = \frac{f_0}{f_2 - f_1}. \quad (3)$$

For the sake of clarity, the rest of the analysis is explained on Fig. 4. From point  $A$  two straight lines are drawn at  $45^\circ$  to the line  $\overline{AS_0}$ , and a third line perpendicular to  $\overline{AS_0}$ . These three straight lines are denoted  $l_3$ ,  $l_4$  and  $l_5$ . The symmetry line between points  $F_\infty$  and  $A$  is drawn afterwards. The

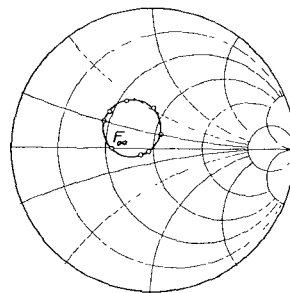


Fig. 1—Typical plot of the input reflectance of a resonator with coupling losses.  $F_\infty$  is the reflectance of the detuned resonator.

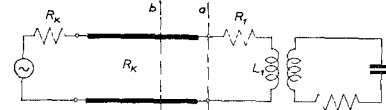


Fig. 2—Equivalent circuit of a resonator with coupling losses.  $a-a$  is the input terminals plane,  $b-b$  is the detuned short plane.

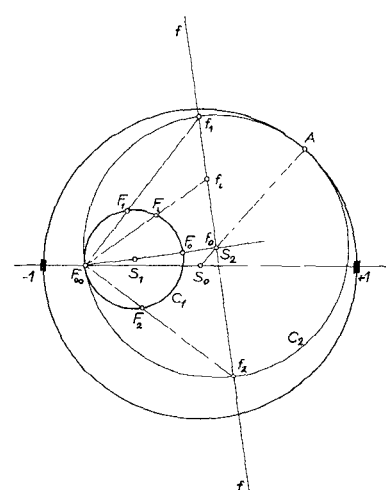


Fig. 3—Input reflectance in the detuned short plane (circle  $C_1$ ). The radii of circles  $C_1$  and  $C_2$  determine the coupling coefficient. Also shown is the construction of a linear frequency scale.

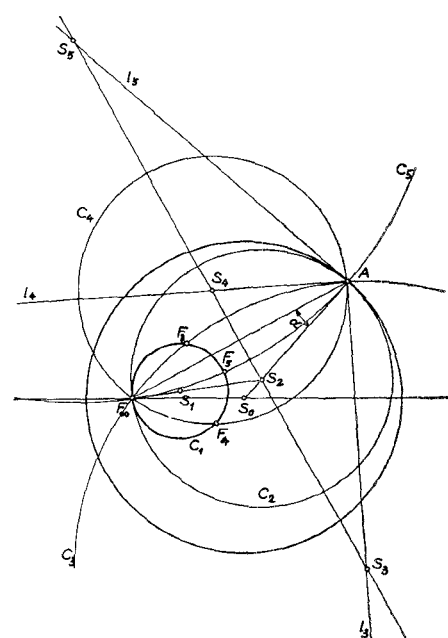


Fig. 4—The determination of the  $Q_0$  and  $f_0$ .

crossings of this line with the lines  $l_3$ ,  $l_4$  and  $l_5$  are  $S_3$ ,  $S_4$  and  $S_5$ . These points are centers of the circles  $C_3$ ,  $C_4$  and  $C_5$  passing through the points  $F_\infty$  and  $A$ .

To obtain a measure for the reactance of the external circuit, we define

$$Q_1 = \frac{\omega L_1}{R_1 + R_K}, \quad (4)$$

the value of which is determined by the radii  $r_2$  and  $r_5$  as follows:

$$Q_1 = \frac{r_2}{r_5}. \quad (5)$$

For small values of  $Q_1$  the point  $S_5$  falls far outside the Smith Chart, and it is therefore more convenient to determine  $Q_1$  from the angle  $\alpha$ .

$$Q_1 = \operatorname{tg} \alpha. \quad (6)$$

The crossings of the circles  $C_3$ ,  $C_4$  and  $C_5$  with the  $Q$  circle  $C_1$  are the points  $F_3$ ,  $F_4$  and  $F_5$ . The corresponding frequencies  $f_3$ ,  $f_4$  and  $f_5$  are found on the frequency scale. The  $Q$  value of the unloaded resonator is then given by

$$Q_0 = \frac{f_5}{f_4 - f_2}. \quad (7)$$

The frequency  $f_5$  is the resonant frequency of the unloaded resonator. Of course,  $Q_0$  may be evaluated also from

$$Q_0 = (1 + \kappa)Q_L. \quad (8)$$

As it can be seen, the described method permits the evaluation of resonator parameters by a straightforward graphical analysis on the Smith Chart. There is, therefore, no need for auxiliary diagrams, which are necessary in the other existing methods<sup>2-4</sup>.

The limitation of the described method consists in the fact that it is usable only in cases where the losses in the coupling circuit can be represented by a series resistance only. It is possible, however, to modify the method also for such cases where the losses are represented by a parallel resistance only. The method becomes rather complicated if the losses are to be represented by a combination of series and parallel resistance.<sup>5</sup>

DARKO KAJFEŽ  
Institute of Automation  
Ljubljana, Yugoslavia

### Calculating Coaxial Transmission-Line Step Capacitance\*

As a frequent user of the curves given by J. R. Whinnery, H. W. Jamieson and T. E. Robbins,<sup>1</sup> I found it useful to arrive at a simple polynomial in powers of  $\alpha$  and  $\tau$ , which makes it possible to incorporate the

TABLE I

	Step on Inner		
	$a_i$	$b_i$	$c_i$
$i=1$	-0.771	+12.6	+ 58.2
2	+1.49	-23.8	-100.0
3	-0.778	+13.1	+ 27.7
4	+0.041 9	- 1.53	+ 15.5
5	+0.000 92	+ 0.069 9	- 0.726

	Step on Outer		
	$a_i$	$b_i$	$c_i$
$i=1$	-0.606	-4.100	+ 82.0
2	+1.13	+3.63	-138.6
3	-0.482	-1.36	+ 48.6
4	-0.115	+1.92	+ 10.2
5	+0.024 0	-0.182	- 0.397

step-capacitance calculation in a subroutine in a computer program dealing with transmission line calculations in coaxial lines.

From considering the peculiarities of the curves (Fig. 8, and Fig. 9 in the above mentioned article), the following form was chosen:

$$\begin{aligned} c'_d = & (a_1 \tau^2 + b_1 \tau + c_1) \alpha^2 \\ & + (a_2 \tau^2 + b_2 \tau + c_2) \alpha^1 + \dots \\ & + (a_5 \tau^2 + b_5 \tau + c_5) \alpha^{-2} \text{ mpf/cm.} \end{aligned}$$

The coefficients for both cases (step on inner, step on outer) are given in Table I. These coefficients give a perfect fit at points  $\alpha = 0.1, 0.3, 0.5, 0.7, 0.9$ , and  $\tau = 1, 3, 5$ , and yield an accuracy of "line thickness" at any other point between the limits  $0.1 \leq \alpha \leq 1.0$ ,  $1 \leq \tau \leq 5$ .

P. I. SOMLO  
Div. of Applied Physics  
National Standards Lab.  
C.S.I.R.O.  
Australia

The primary purpose of loading a small scatterer is to increase its echo area. The general formula is given by (18) of Harrington,<sup>1</sup> but in most cases the second term is large compared to the first term. Also, by reciprocity, the  $B$  of (18) is the scatterer gain times its input resistance; hence

$$\frac{\sigma}{\lambda^2} \approx \frac{1}{\pi} \left| \frac{GR_{in}}{Z_{in} + Z_L} \right|^2, \quad (1)$$

where  $\sigma$  = echo area,  $\lambda$  = wavelength,  $Z_{in} = R_{in} + jX_{in}$  = the input impedance of the scatterer when used as an antenna,  $G$  is the directive gain of the scatterer when used as an antenna, and  $Z_L$  is the load impedance connected to the scatterer terminals. Note that the echo area is completely determined by the characteristics of the scatterer when used as an antenna. The extension of (1) to the case of bistatic scattering involves merely the replacement of  $G^2$  by  $G_1 G_2$ , where  $G_1$  is the gain in the direction of the source and  $G_2$  is the gain in the direction of the receiver.

By using a negative resistance load, one can make the denominator of (1) arbitrarily small, obtaining very large echo areas from small scatterers. In practice, the maximum echo area is limited by instabilities that arise. Some of the characteristics of small scatterers with negative resistance loads that are of importance in field measuring techniques are as follows. 1) The scatterer becomes extremely sensitive to proximity effects, because a small change in  $Z_{in}$  results in a large change in  $\sigma$ . Hence, such scatterers might be useful for the measurements in regions distant from objects, but probably not close to objects. 2) The scatterer behaves similarly to a resonant circuit with an effective quality factor

$$Q = \frac{|X_{in}|}{R_{in} + R_L}, \quad (2)$$

which becomes very large when  $R_L$  is negative. Hence, the scatterer becomes a very narrow-band device. This may be an advantage if a frequency-modulated system is used, as discussed in Sec. VIII of Harrington.<sup>1</sup> 3) Because the scatterer behaves as a resonant circuit, it can be shown that a scatterer is characterized by a constant gain-bandwidth product, that is,

$$\sigma \beta^2 = \text{constant}, \quad (3)$$

where  $\beta$  = fractional frequency bandwidth between points where  $\sigma$  has fallen to  $1/2$  its value at resonance. Fig. 1 illustrates this

### Field Measurements Using Active Scatterers\*

A general theory for analyzing scattering from loaded scatterers is available, and has been applied to small scatterers suitable for electromagnetic field measurements.<sup>1</sup> The theory is valid for both passive and active loads, as long as the load is linear. Ryerson has proposed the use of tunnel diodes to provide a negative resistance load, thereby enhancing the scattered signal.<sup>2</sup> His predictions have been verified experimentally by measurements on dipoles and tunnel diodes at  $S$  band.<sup>3</sup> The use of scatterers and tunnel diodes for field measurements is discussed in this communication.

\* Received April 26, 1963. The work reported here was supported by Rome Air Development Center order Contract No. AF 30(602)-2900.

<sup>1</sup> R. F. Harrington, "Small resonant scatterers and their use for field measurements," *IRE TRANS. ON MICROWAVE THEORY AND TECHNIQUES*, vol. MTT-10, pp. 165-174, May, 1962.

<sup>2</sup> J. L. Ryerson, "Scatter echo area enhancement," *PROC. IRE (Correspondence)*, vol. 50, p. 1979, September, 1962.

<sup>3</sup> J. Forgione, E. Calucci, and C. Blank, "The Application of Tunnel Diodes to a Reflecting Antenna Array," *Applied Research Lab., Rome Air Development Center, Griffiss Air Force Base, N. Y.*, T.D. Rept. No. RADC-TDR-63-4; January, 1963.

\* Received June 5, 1963.

<sup>1</sup> J. R. Whinnery, H. W. Jamieson, and T. E. Robbins, "Coaxial line discontinuities," *PROC. IRE*, vol. 32, pp. 695-709; November, 1944.